LA-UR-19-26647
Approved for public release; distribution is unlimited.

Title: Multiple Phase Screen Scintillation Modeling Code

Author(s): Light, Max Eugene

Intended for: Report

Issued: 2019-07-15

Multiple Phase Screen Scintillation Modeling Code

Max Light

July 12, 2019

Abstract

This document describes the underlying theory and use of a computer code written to simulate scintillation effects on propagating electromagnetic (EM) signals. The Multiple Phase Screen (MPS) technique [1, 2, 3, 4] is employed to model the effects of scintillation on EM signals as they travel through the earth's ionosphere.

Contents

Introduction

The phenomenon of random fluctuations in the amplitude and phase of received transionospheric radio frequency (RF) signals is well known and documented [5]. Earliest observations occurred during monitoring of 64 MHz radiation from the radio star Cygnus [6]. It was initially thought that the observed fluctuations in the received signal were due to the radio star itself. However, later observations showed no correlation between the signal received at stations 210 km apart, whereas the received signal at stations only 4 km apart was well correlated, revealing the local nature of the signal fading.

For wide band signals, sometimes a part or even the whole band can suffer degredation or complete drop out at the receiver. The former is known as frequency selective scintillation where only a fraction of the signal bandwidth is affected, whereas the latter is know as flat fading.

As a physical process, scintillation is best described as random variations in the amplitude and phase of a propagating EM wave caused by an irregular structure in the local electron density [2]; or equivalently, diffraction of the EM wave due to spatial irregularities in the electron content in the ionosphere.

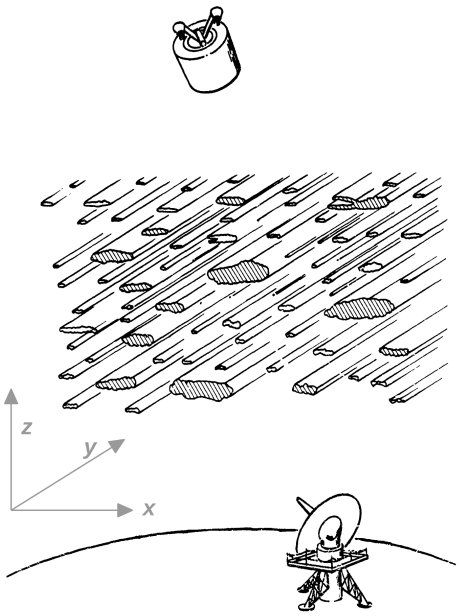

Figure 1.1: Conditions and geometry for transionospheric signal scintillation, from [2].

In the ionosphere, irregular electron density structure is caused by plasma instabilities which distribute the electron density randomly along local magnetic field lines. Thus, a striated plasma forms with rods, or sheets, of increased (or decreased) plasma density relative to the surrounding background plasma (see Fig. 1.1). These electron density fluctuations effectively create a stochastic 'screen' that causes the phase of the incident signal, at that location along the screen, to advance or retard in a fashion governed by the spatial statistics of the density fluctuations. Signal scintillation can be characterized from one or more of these phase screens.

This *diffraction* is different from the *refraction* experienced by the EM wave as it propagates through the bulk magnetized plasma. Think of the situation as EM wave propagation through a background media that has a quiescent, or bulk, characteristic with a stochastic component superimposed. The EM wave will refract through the bulk, and also suffer diffraction due to the stochastic part.

Naturally, the scintillation suffered by a propagating EM wave with polarization along or across

the magnetic field will be different.

For wide bandwidth signals, each frequency component experiences a different phase perturbation through the same region due to the dispersive nature of EM wave propagation through a plasma. The time variation in the plasma irregularities will also affect the imparted phase.

EM wave propagation through a 'disturbed' ionosphere, then, can be described in two parts. In the first, wave refraction through the quiescent (bulk) plasma is calculated using standard techniques such as full wave solutions or ray tracing techniques [7, 8, 9, 10]. The second part is the calculation of the propagation characteristics through the stochastic component of the ionospheric electron density [2, 3, 4, 11]. The solutions for the propagating wave fields in each part can then be added.

This report describes the development and implementation of an MPS-based scintillation model to predict the behavior of EM waves as they propagate through a disturbed ionosphere.

Theory

The material that follows draws heavily from Knepp [2, 3].

As outlined in section 1, scintillation effects on propagating EM waves (also referred to herein as RF signals, or simply signals) are best described as diffraction through a screen, or screens, with a stochastic grid(s) created by instabilities that randomly distribute ionospheric plasma electrons with structure along and across the local magnetic field (figure 1.1). The phase imparted to the signal, along the grid, will have different statistical properties depending on the orientation of electric field with respect to the local magnetic field.

2.1 EM wave propagation

We are interested in the propagation characteristics of the signal as it travels through a stochastic medium. It's propagation characteristics due to the quiescent background medium (a plasma for our case) we can assume have already been determined. Because of this, we can consider that EM wave as propagating through free space and encountering one or more phase screens whose properties are derived from the stochastic component of the plasma medium. The solution for the wave fields for both cases can then be superimposed.

2.1.1 Parabolic wave equation

Start with the wave electric field equation for plane, time harmonic electromagnetic waves propagating through free space

$$\nabla^2 \vec{E} + k_0^2 n^2 \vec{E} = 0 \tag{2.1}$$

where $\vec{E} \propto E(\vec{r})e^{i(\vec{k}\cdot\vec{r}-\omega t)}$, the free space wave number is $k_0^2 = \omega^2/c^2$ at frequency ω, c is the speed of light, and the index of refraction of the medium is n. From this point forward, the time dependence $e^{-i\omega t}$ will be dropped for convenience.

The geometry of the problem separates naturally into directions parallel and perpendicular to the magnetic field B_0. Thus, we can treat the stochastic part of the plasma as non-magnetized with different statistical properties along, or across B_0. Electric field polarization can effectively be separated in this manner without loss of generality. With this in mind, we assume propagation in the z direction (up) with plasma gradients in x and y. Parallel to B_0 in y, we expect gradients to be very gradual. We will thus solve the problem in the $z-x$ plane (figure 1.1), where all gradients are assumed across the magnetic field (x). Under this approximation, we expect to use statistics of the stochastic plasma perpendicular to B_0.

We will assume plane wave propagation mostly in z, also known as the parabolic approximation, so that the wave electric field can be written as

$$E(x,z,\omega) = U(x,z,\omega)e^{-ikz} \tag{2.2}$$

This is equivalent to stating that the wave propagates mostly in one direction. The medium through which the wave travels is free space with a perturbation due to the stochastic part of the background plasma (recall that we assume the propagation characteristics of the EM wave through the quiescent background plasma have already been solved). The index of refraction of an unmagnetized plasma is [9, 8]

$$n = \sqrt{1 - \omega_p^2/\omega^2} \tag{2.3}$$

where the plasma frequency is defined as $\omega_p^2 = n_e e^2/(\epsilon_0 m_e)$, where ϵ_0 is the permittivity of free space, the local plasma electron density is n_e, and m_e is the electron mass. Assuming a frequency far enough above ω_p, the index of refraction is then

$$n = \sqrt{1 - \omega_p^2/\omega^2} \;\simeq\; 1 - \frac{1}{2}\frac{n_e e^2}{\epsilon_0 m_e} = 1 - \frac{1}{2}\frac{n_e \lambda^2 r_e}{\pi} \tag{2.4}$$

where r_e is the classical electron radius given by [12]

$$r_e = \frac{e^2}{\epsilon_0 m_e 4\pi c^2} \tag{2.5}$$

The index of refraction now consists of a background free space part and a perturbation due to the plasma Δn

$$n = 1 + \Delta n \tag{2.6}$$

$$= 1 - \frac{1}{2}\frac{\lambda^2 r_e}{\pi}\Delta n_e \tag{2.7}$$

such that

$$\Delta n = -\frac{1}{2}\frac{\lambda^2 r_e}{\pi}\Delta n_e \tag{2.8}$$

The wave equation (Eq. 2.1) is then

$$\nabla^2 \vec{E} + k_0^2 \vec{E} - k_0^2 \frac{\lambda^2 r_e}{\pi}\Delta n_e \vec{E} = 0 \tag{2.9}$$

and using Eq. 2.2 it becomes

$$\frac{\partial^2 U}{\partial x^2} - i2k_0\frac{\partial U}{\partial z} + \frac{\partial^2 U}{\partial z^2} - k_0^2\frac{\lambda^2 r_e}{\pi}\Delta n_e U = 0 \tag{2.10}$$

We further impose the condition of nearly parallel (in z) propagation as

$$\left|2k_0\frac{\partial U}{\partial z}\right| >> \left|\frac{\partial^2 U}{\partial z^2}\right| \tag{2.11}$$

That is, U is a slowly varying function of z and changes only over the scale size l such that $k \sim 1/\lambda$, $\partial U/\partial z \sim 1/l$ and $l >> \lambda$. Under that constraint, the parabolic wave equation for a plane

wave traveling in a mostly un-deflected manner through a background of free space with plasma perturbations is finally

$$\frac{\partial^2 U}{\partial x^2} - i2k_0\frac{\partial U}{\partial z} - k_0^2\frac{\lambda^2 r_e}{\pi}\Delta n_e U = 0 \tag{2.12}$$

To solve for signal propagation through a region described by equation 2.12, we can describe it as being comprised of one or more thin layers of plasma , each layer being perpendicular to the direction of propagation, with free space between them.

2.1.1.1 Inside plasma layer

Consider a layer whose thickness is Δz. If Δz is small, the equation to describe wave propagation is taken from equation 2.12 with the first term neglected. That is, we neglect the free-space propagation term relative to the plasma one.

$$i2k_0\frac{\partial U}{\partial z} + k_0^2\frac{\lambda^2 r_e}{\pi}\Delta n_e U = 0 \tag{2.13}$$

This differential equation is easily solved to give

$$U\left(x, \Delta z/2\right) \;=\; U\left(x, -\Delta z/2\right) \cdot \exp\left[-ir_e\lambda\int_{-\Delta z/2}^{\Delta z/2}\Delta n_e(x,z)dz\right] \tag{2.14}$$

2.1.1.2 Between plasma layers

Between the phase screen layers, the medium through which the signal travels is free space. This is corectly described by equation 2.12 if the third term is dropped

$$\frac{\partial^2 U}{\partial x^2} - i2k_0\frac{\partial U}{\partial z} = 0 \tag{2.15}$$

The solution to this equation is found by using the Fourier transform of the field in the direction perpendicular to the propagation, and then advancing the field in the propagation direction as in equation 2.13

$$\frac{\partial^2 \widehat{U}(k_\perp, z)}{\partial x^2} - i2k_0\frac{\partial \widehat{U}(k_\perp, z)}{\partial z} = 0 \tag{2.16}$$

where the Fourier transform pair is defined as

$$\widehat{U}(k_\perp, z) \;=\; \frac{1}{2\pi}\int_{-\infty}^{\infty} U(x,z)e^{-ik_\perp x}dx \tag{2.17}$$

$$U(x,z) \;=\; \int_{-\infty}^{\infty}\widehat{U}(k_\perp, z)e^{+ik_\perp x}dk_\perp \tag{2.18}$$

Using equations 2.17 and 2.18 in 2.16, the propagated wave field solution from z_1 to z_2 is

$$U(x,z_2) \;=\; \mathfrak{F}^{-1}\left[\widehat{U}(k_\perp, z_1)\exp\left\{ik_\perp^2(z_2-z_1)/2k_0\right\}\right] \tag{2.19}$$

$$\;=\; \int_{-\infty}^{\infty}\widehat{U}(k_\perp, z_1)\exp\left\{ik_\perp^2(z_2-z_1)/2k_0 + ik_\perp x\right\}dk_\perp \tag{2.20}$$

where $\mathfrak{F}[\,]$, $\mathfrak{F}^{-1}[\,]$ denote the Fourier transform and inverse transform of their argument respectively. The term $\exp\left\{ik_\perp^2(z_2-z_1)/2k_0\right\}$ is known as the *Fresnel propagator* - essentially a filter function applied to $\widehat{U}(k_\perp, z_1)$ in k-space.

2.1.1.3 Parabolic wave equation solution

Propagation of an EM wave from one z location to another through free space and a series of phase screens is then accomplished using equations 2.14 and 2.19 using the 'split step' algorithm. Start with a plane wave incident on the first phase screen. Only the phase of the emergent EM electric field is affected by the screen according to equation 2.14. The field is then Fourier transformed from $E(x,z)$ to $\widehat{E}(k_\perp,z)$ immediately after the screen, and propagated to the next screen through free space via equation 2.19. This step is accomplished by multiplying $\widehat{E}$ by $\exp[ik_\perp^2(z_2-z_1)/2k_0]$, for traveling a distance z_2-z_1, and then taking its inverse Fourier transform. The process starts again at the next phase screen until the EM wave has propagated the required distance.

This solution technique effectively replaces this *diffractive* effects of the ionosphere by a series of phase screens. The *refractive* effects, as outlined earlier, are solved using standard full wave or ray tracing techniques. The full solution is a superposition of the two.

2.1.2 Phase screen realization

The phase screens implemented in the split step solution outlined above are constructed with a priori knowledge of the statistics of the stochastic part of the ionospheric plasma electron density irregularities $\Delta n_e(x,z)$. It is necessary, then, to connect these statistics to the actual value of phase imparted to the wave at each x location along the screen. The statistics of the electron density irregularities can be quantified by their power spectral density (PSD) as a function of perpendicular wavelength ($\lambda_x \Leftrightarrow k_\perp$) along the grid. And it is this PSD that we can relate to the PSD of the phase $\phi(x)$. To find this relationship, start with the equation for the phase contribution along the grid from equation 2.14, that phase component is given by

$$\phi(x) = -ir_e\lambda \int_{-\Delta z}^{\Delta z} \Delta n_e(x,z)dz \tag{2.21}$$

In what follows, the stochastic electron density fluctuations are assumed to be zero mean and statistically stationary [13, 11].

2.1.2.1 Statistical relationships - phase contribution along screen

The phase autocorrelation function is constructed as

$$\begin{aligned} B_\phi(\xi) &= \langle \phi(x)\phi^*(x+\xi)\rangle & (2.22)\\ &= r_e^2\lambda^2 \int_{-\Delta z/2}^{\Delta z/2}\int_{-\Delta z/2}^{\Delta z/2} \langle \Delta n_e(x,z)\Delta n_e(x+\xi,z')\rangle\, dzdz' & (2.23)\end{aligned}$$

where the brackets <> represent ensemble averages. The integrand in equation 2.23 is the autocorrelation function of the electron density fluctuations

$$B_{n_e}(\xi, z-z') = \langle \Delta n_e(x,z)\Delta n_e(x+\xi,z')\rangle \tag{2.24}$$

This double integral can be reduced to a single integral using a change of variables [14] to get

$$B_\phi(\xi) = r_e^2\lambda^2\Delta z \int_{-\Delta z}^{\Delta z} \left(1-\frac{|z'|}{\Delta z}\right) B_{n_e}(\xi,z')dz' \tag{2.25}$$

If the phase screen thickness Δz is greater than the correlation length of the electron density fluctuations, the contribution of the second term in equation 2.25 is always neglibible, and the limits can be extended

$$B_\phi(\xi) = r_e^2 \lambda^2 \Delta z \int_{-\infty}^{\infty} B_{n_e}(\xi, z') dz' \tag{2.26}$$

Furthermore, according to the Wiener–Khinchin theorem, under the assumption of wide-sense stationary processes, we know that the Fourier transform of the autocorrelation function of some $f(x)$ is the power spectral density (PSD) of that function. That is

$$S(k) = \frac{1}{2\pi} \int_{-\infty}^{\infty} B(\xi) e^{-ik\xi} d\xi \tag{2.27}$$

Recall that the variable ξ is the separation distance in the perpendicular direction x along the phase screen. We can then Fourier transform $B_\phi(\xi)$ from ξ to $k_\perp$ and use equation 2.26

$$\mathfrak{F}[B_\phi(\xi)] \;=\; S_\phi(k_\perp) \;=\; \frac{r_e^2 \lambda^2 \Delta z}{2\pi} \int_{-\infty}^{\infty} \int_{-\infty}^{\infty} B_{n_e}(\xi, z') e^{-ik_\perp \xi} dz' d\xi \tag{2.28}$$

This equation is the relation between the one dimensional PSD of the phase fluctuations and the two dimensional autocorrelation function of the electron density fluctuations. The Fourier transform relationship between the two dimensional PSD and autocorrelation functions relevant to equation 2.28 is [2]

$$S(k_x, k_y) = \frac{1}{4\pi^2} \int_{-\infty}^{\infty} \int_{-\infty}^{\infty} B(x, y,) e^{-i(k_x x + k_y y)} dx dy \tag{2.29}$$

So that we now obtain

$$S_\phi(k_\perp) \;=\; 2\pi r_e^2 \lambda^2 \Delta z \cdot S_{n_e}(k_\perp, k_z = 0) \tag{2.30}$$

With this equation, we have 'closed the loop' from the *two dimensional* statistics of the stochastic electron density fluctuations and the *one dimensional* phase fluctuations imparted along the phase screen. We can go one step further to get one dimensional statistics for each side.

Note that in equation 2.30, the PSD of the electron density fluctuations is evaluated at $k_z = 0$. This implies that we are taking the spectrum of vertically integrated density fluctuations [15], which are just the vertical total electron content (TEC) fluctuations, and these can be measured more readily than the local electron density. In a more general sense, 'vertical' means perpendicular to the propagation direction of the wave. Take equation 2.23 and perform the integration in z

$$B_\phi(\xi) = r_e^2 \lambda^2 \left\langle \Delta TEC(x)\ \Delta TEC(x+\xi) \right\rangle \;=\; r_e^2 \lambda^2 B_{TEC}(\xi) \tag{2.31}$$

and again use the Wiener–Khinchin theorem (equation 2.28). We finally arrive at the one dimensional relation

$$S_\phi(k_\perp) \;=\; r_e^2 \lambda^2 \cdot S_{TEC}(k_\perp) \tag{2.32}$$

or, in terms of the Fourier amplitudes of each PSD, keeping in mind that $k_\perp$ is always real,

$$\left| \widehat{\phi}(k_\perp) \right|^2 = r_e^2 \lambda^2 \cdot \left| \widehat{\Delta TEC}(k_\perp) \right|^2 \tag{2.33}$$

This important result relates the statistics of the phase content imparted to the wave as it encounters a phase screen to the statistics of the TEC fluctuations at locations along the screen. These

statistics are given in a direction perpendicular to the wave's propagation direction and must be specified carefully, for example, along or across the local magnetic field. If we can thus specify the PSD of the TEC fluctuations, we can relate it directly to the phase contribution fluctuation PSD and use the Fourier inverse transform to directly solve for those contributions along the screen

$$\phi(x) = \mathfrak{F}^{-1}\left[\sqrt{S_\phi(k_\perp)}\right] \tag{2.34}$$

Using this result, equations 2.14 and 2.19, are modified to accommodate the split step algorithm solution for the wave fields under parabolic wave equation

inside phase screen

$$U\left(x, \Delta z/2\right) = U\left(x, -\Delta z/2\right) \cdot \exp\left[-i\mathfrak{F}^{-1}\left[\sqrt{S_\phi(k_\perp)}\right]\right] \tag{2.35}$$

between phase screens

$$U(x, z_2) = \mathfrak{F}^{-1}\left[\widehat{U}(k_\perp, z_1)\exp\left\{ik_\perp^2(z_2 - z_1)/2k_0\right\}\right] \tag{2.36}$$

where the phase screen is Δz thick, and the distance traveled by the wave in free space is $z_2 - z_1$.

2.1.2.2 Statistical relationships - ΔTEC and phase variances

Consider the Wiener–Khinchin theorem as stated in equation 2.27

$$S(k) = \mathfrak{F}[B(\xi)] \tag{2.37}$$

The inverse Fourier transform gives

$$B(\xi) = \mathfrak{F}^{-1}[S(k)] = \int_{-\infty}^{\infty} S(k)e^{ik\xi}dk \tag{2.38}$$

In general, the evaluation of the autocorrelation function at 0 gives the variance, thus

$$B(\xi = 0) = \sigma^2 = \int_{-\infty}^{\infty} S(k)dk \tag{2.39}$$

Using this result in equation 2.32 gives an important relationship between the phase and TEC variances

$$\sigma_\phi^2 = r_e^2\lambda^2\sigma_{TEC}^2 \tag{2.40}$$

which will be used in the implementation of the split step algorithm to 'calibrate' the phase PSD function $S_\phi(k_\perp)$ in equation 2.35 using the statistics of the TEC parameter.

Computer Algorithm

In this section, the solution of the parabolic wave equation using the split step technique will be outlined. The approach is a straightforward application of equations 2.35 and 2.36.

3.1 Overview

To start, the time representation of the signal, $f(t)$, to be propagated is supplied. It is represented as a plane wave by assigning a copy of the waveform to each (perpendicular to the direction of propagation) location along the screen, forming a two dimensional 'plane wave array' (PWA) in time and space. The time dimension is then Fourier transformed to frequency to get the spectral components of the signal at each screen location.

The next step is to impart a phase representing the stochastic fluctuation statistics of the TEC fluctuations at each location to its corresponding copy at the same location. This is done via equation 2.35 and knowledge of the TEC fluctuation statistics, which will be discussed later. For now, assume the phase screen spatial distribution, $\phi_0(x)$, has already been calculated from the TEC fluctuations at a frequency specified as the center frequency, f_0, in the bandwidth of the original signal. The corresponding phase shift imparted to the concomitant waveform along the screen as a function of x and frequency is then [2]

$$\phi_f(x) = \frac{f_0}{f} \cdot \phi_0(x) \tag{3.1}$$

In this way, the phase contribution to the waveform is applied along the corresponding frequency and space dimension of the PWA.

Once the contribution from the phase screen has been imposed on the wave, it must be propagated a distance Z to either the next screen, or to the receiver (note that the distance $Z = 0$ is also valid, implying that the waveform experiences only a single screen). The Fourier transform from equation 2.36 is applied along the space dimension of the PWA whose dimensions are now frequency and wave number. Recall that numerically, the perpendicular wave number used in the algorithm corresponds to the x locations along the grid, such that for n evenly spaced locations at intervals of Δx, we have the perpendicular wave number increment

$$\Delta k_\perp = \frac{2\pi}{n \cdot \Delta x} \tag{3.2}$$

and this is used in the factor $\exp\{ik_\perp^2(z_2 - z_1)/2k_0\}$ which is multiplied along the corresponding wave number dimension of the PWA.

The inverse Fourier transform along the wave number dimension is applied to bring the PWA back to frequency and space dimensions, and the process is repeated until the receiver has been reached.

3.2 Numerical phase screen generation

The accuracy of the MPS split step solution of the parabolic wave equation depends on how the phase is imparted along the perpendicular phase screen. This is a stochastic process and as such, single solutions for the propagating wave fields are only representative of the overall TEC fluctuation statistics based on that particular realization of the phase screen. In other words, a single wave field/phase screen solution is not as important as the *statistics* of an ensemble of wave field/phase screen solutions.

With that in mind, we wish to generate a phase screen that is a statistically stationary random function $\phi(n \cdot \Delta x)$ which represents the phase contribution along the screen at the nth location of even intervals Δx.

3.2.1 GRV filter function

If the stochastic phase PSD $S_\phi(k_\perp)$ were known, then the phase contribution along the grid is given by the Fourier transform

$$\phi(x) = \mathfrak{F}^{-1}\left[\widehat{\phi}(k_\perp)\right] = \mathfrak{F}^{-1}\left[\sqrt{S_\phi(k_\perp)}\right] \tag{3.3}$$

With knowledge of the functional form of $S_\phi(k_\perp)$, we can construct a digital version by applying a filtering function to a Gaussian random variable (GRV) in perpendicular wave number space.

$$\widehat{\phi}_d(k_\perp) = \sqrt{S_{\phi,d}(k_\perp)} = \mathfrak{r} \cdot \sqrt{S_\phi(k_\perp)\frac{L}{2\pi}} \tag{3.4}$$

where the subscript d denotes the numerically calculated value, L is the phase screen length, and $\mathfrak{r}$ is a complex number formed from the sum of two independent Gaussian random variables with unity variance and zero mean [2].

$$\mathfrak{r} = \sqrt{\frac{1}{2}} \cdot (\mathfrak{g}_1 + i\mathfrak{g}_2) \tag{3.5}$$

Since the phase of a single phase screen realization is a real quantity, either the real or imaginary part of $\mathfrak{r}$ can be chosen. The particular choice of the GRV filtering function $\widehat{\phi}_d(k_\perp)$ given in equation 3.4 will now be justified. We have initially required that the stochastic fluctuations be statistically stationary, thus ensemble averages or expectations of random quantities can be replaced by spatial averages. The phase autocorrelation of $\phi_d(x)$ from equation 2.22 can be written as

$$B_{\phi,d}(\xi) = \langle \phi_d(x+\xi)\phi_d^*(x)\rangle \tag{3.6}$$

$$= \frac{1}{L}\int_0^L \phi_d(x+\xi)\phi_d^*(x)dx \tag{3.7}$$

with equations 3.3 and 3.4, this results in

$$B_{\phi,d}(\xi) = \frac{1}{L}\int_0^L dx \int_{-\infty}^{+\infty} dk_\perp \int_{-\infty}^{+\infty} dk'_\perp \mathfrak{r}\mathfrak{r}^* \frac{L}{2\pi}[S_{\phi,d}(k_\perp)]^{1/2}[S'^*_{\phi,d}(k'_\perp)]^{1/2} e^{ik_\perp x} e^{-ik'_\perp x} e^{i\xi x} \tag{3.8}$$

recall that

$$2\pi \int_{-\infty}^{+\infty} e^{ix(k_\perp - k'_\perp)} dx = \delta(k_\perp - k'_\perp) \tag{3.9}$$

so that equation 3.8 becomes

$$B_{\phi,d}(\xi) = \int_{-\infty}^{+\infty} dk_\perp S_{\phi,d}(k_\perp) e^{ik_\perp x} |\mathfrak{r}|^2 dk_\perp \tag{3.10}$$

Comparing this result with equations 2.38 and 3.4 it is apparent that the choice of the GRV filter function gives the PSD of the *numerically* generated $S_{\phi,d}(k_\perp)$ gives the original $S_\phi(k_\perp)$ multiplied by the sum of the squares of two Gaussian random variables ($|\mathfrak{r}|^2$). Thus, for any particular phase screen realization $S_{\phi,d}(k_\perp)$ will not be identical to $S_\phi(k_\perp)$. However, the ensemble average of many realizations of $S_{\phi,d}(k_\perp)$ will go to $S_\phi(k_\perp)$ since $< |\mathfrak{r}|^2 >= 1$.

3.2.2 Calibration of $S_\phi(k_\perp)$

Knowledge of the ΔTEC fluctuation PSD gives the phase screen contribution along the screen via equations 2.32 and 2.34

$$\phi(x) = r_e \lambda \cdot \mathfrak{F}^{-1} \left[\sqrt{S_{TEC}(k_\perp)} \right] \tag{3.11}$$

This method of generating a random phase screen given the functional form of $S_{TEC}(k_\perp)$ has been shown to be correct in [2].

There are many different forms of $S_\phi(k_\perp)$ (that is, $r_e^2 \lambda^2 S_{TEC}(k_\perp)$) in the literature [16, 5, 4], however, we are interested in the ability to fit a general functional form to $S_\phi(k_\perp)$ for use in the MPS wave field solution. This enables investigation into local TEC fluctuations that might be driven by specific scale length disturbances, as well as more general background fluctuations. To do this, we need to 'calibrate' the wave number filter function $\widehat{\phi}_d(k_\perp)$ in equation 3.4 so that it has the proper magnitude in wave number space. Thus we can say

$$S_{TEC}(k_\perp) = Q \cdot f(k_\perp) \tag{3.12}$$

where Q is a normalization parameter. Consider the relation between the variance and the integral of the PSD in equation 2.39 and the relationship between the phase and TEC fluctuations in equation 2.40. We find Q using those two equations

$$Q = \frac{\sigma_{TEC}^2}{\int_{-\infty}^{\infty} f(k_\perp) dk_\perp} \tag{3.13}$$

Then, from equation 2.40

$$Q \cdot \int_{-\infty}^{\infty} f(k_\perp) dk_\perp = r_e^2 \lambda^2 \int_{-\infty}^{\infty} S_\phi(k_\perp) dk_\perp \tag{3.14}$$

or

$$S_\phi(k_\perp) = \frac{Q}{r_e^2 \lambda^2} f(k_\perp) \tag{3.15}$$

Thus, *with a priori knowledge of the variance of the TEC fluctuations*, σ_{TEC}^2, we have the GRV filter function from equations 3.4 and 3.15

$$\widehat{\phi}_d(k_\perp) = \mathfrak{r} \cdot \frac{\sqrt{Q f(k_\perp)}}{r_e \lambda} \tag{3.16}$$

3.3 Region of validity for MPS application

Overall, we are calculating the magnitude and phase of the propagating plane wave field at a discrete number of points along the phase screen, and then propagating them to the next screen or to a receiver. To do this, we are required to take Fourier transforms in both time ($t \Leftrightarrow \omega$) and space ($\lambda \Leftrightarrow k$). This and the discrete nature of the calculation imposes restrictions on the number and spacing between the points [16, 2], these are:

phase representation The phase screen must adequately represent the actual phase.

wave propagation The wave should propagate without angular aliasing.

edge effects Edge effects or 'angular scattering' off the ends of the phase screen grid must be minimal.

3.3.1 Phase representation

The change in phase between adjacent points on the phase screen must be less than π. That is, for the n^{th} point on the grid

$$\phi(x_{n+1}) - \phi(x_n) < \pi \qquad \text{or} \qquad \Delta x \left| \frac{d\phi(x)}{dx} \right| < \pi \tag{3.17}$$

In terms of the overall number of points along the grid, a good rule of thumb [2] is

$$\Delta x < \frac{l_i}{3} \tag{3.18}$$

where l_i is the *inner scale*, that is, the smallest spatial length of stochastic fluctuations represented in $S_\phi(k_\perp)$. A further constraint on the grid size is that it be longer than at least five times the *outer length* L_0 , which is the largest spatial scale size of disturbances represented in $S_\phi(k_\perp)$ [2].

3.3.2 Wave propagation

The wave can propagate only a certain distance before the Nyquist limiting criterion imposed by the Fresnel propagator in equation 2.19 becomes the limiting factor. That is, a distance z,

$$\frac{k_\perp^2 z}{2k_0} < \pi \tag{3.19}$$

when evaluated from one discrete value of $k_\perp$ to the next. This can be further reduced to a tractable constraint. For a screen of length L divided into N points, the maximum value of $k_\perp$ from the Nyquist criterion, and the next lower value are

$$k_{\perp,max} = \frac{N\pi}{L}, \qquad k_{\perp,max-1} = \frac{(N-1)\pi}{L} \tag{3.20}$$

Using these two expressions in their concomitant Fresnel propagators, we get

$$\frac{\pi^2 N^2 z}{2k_0 L^2} - \frac{\pi^2 (N-1)^2 z}{2k_0 L^2} < \pi \tag{3.21}$$

which reduces to

$$z < \frac{2L\Delta x}{\lambda} \tag{3.22}$$

where $k_0 = 2\pi/\lambda$ is the parallel (z) wave number of the propagating plane wave.

3.3.3 Edge effects

Fourier transforms are used to specify energy in the form of TEC fluctuations along the grid, and this energy will fold from one side of the grid to the other due to the periodic nature of the digital Fourier transform (DFT). This effect must be mitigated, especially at large propagation distances (in z) from the grid. The scattering angle of energy as it leaves the grid is given by

$$\theta = \frac{1}{k_0}\frac{d\phi(x)}{dx} \tag{3.23}$$

the energy scattered at an angle θ travels a distance $z\theta$ perpendicular to the direction of wave propagation after the wave travels a distance of z. Thus, for a propagation distance z, we want the grid to extend a distance L greater than $z\theta$ to ensure against edge effects

$$L > z\theta \qquad \text{or} \qquad L > \frac{z}{k_0}\left|\frac{d\phi(x)}{dx}\right| \tag{3.24}$$

Applications

4.1 Verification - Gaussian phase lens

One way to check the validity of the MPS code is to impose a deterministic phase screen to the propagating wave and compare the wave field results to theory. This method is basically a check on the Fresnel propagator used in equation 2.36, but nevertheless is a good first step in code verification.

Here, the MPS code will be applied to a deterministic, non-random, phase screen representing a Gaussian phase lens. The phase screen will impose a phase contribution to the wave as

$$\phi(x) = -\phi_0 \cdot e^{-x^2/r_0^2} \tag{4.1}$$

where $\phi(x)$ is the imparted phase contribution used in the first step of the split step method in equation 2.35. Note that the negative value of $\phi(x)$ corresponds to a positive phase contribution from equation 2.35 causing the screen to act as a focusing lens. Likewise, a positive $\phi(x)$ will create a diverging field.

For this exercise, a single frequency plane wave of 100kHz is subjected to a phase screen of length 128 meters at the propagation origin ($z = 0$). The phase contribution along the grid is specified with the parameters $r_0 = \lambda$ meters and $\phi_0 = 10$ radians.

$$\phi(x) = -10 \cdot e^{-x^2/\lambda^2} \tag{4.2}$$

The focal length for a Gaussian lens is [2, 17]

$$F = \frac{kr_0^2}{2\phi_0} \tag{4.3}$$

or, for $r_0 = \lambda$

$$F = \frac{\pi\lambda}{\phi_0} \tag{4.4}$$

which is $0.314\lambda = 942.5$ meters using the assigned parameters.

The plane wave then propagates a distance beyond the screen at $z = 0$ and the the value of $|E(x,z)|^2$ is calculated. This result can be compared to theory [16, 18] for the propagated E field

$$E(x,z) = \frac{\exp[ik_0(z+x^2)/2z]}{\sqrt{ik_0 z}} \times \sum_{n=0}^{\infty} \frac{(i\phi_0)^n}{n!} \left(\frac{2n}{k_0^2 r_0^2} - \frac{1}{k_0 z}\right)^{-1/2} \times \exp\left(\frac{\frac{-x^2}{2z^2}}{\frac{2n}{k_0^2 r_0^2} - \frac{i}{k_0 z}}\right) \tag{4.5}$$

The results of this comparison are given in figures 4.2, 4.3, 4.4, and 4.5.

Figure 4.2 shows the E-field intensity $|E|^2$ as it travels away from the screen. The agreement between the MPS code and theory is excellent except at a distance of 30 wavelengths from the screen. At this point, both edge effects due to the finite size of the phase screen (equation 3.24) and wave propagation distortion due to the Fresnel propagator (equation 3.22) are significant contributors to the field intensity. These effects are also seen in figures 4.4 and 4.5.

IT is also evident from figure 4.2 that the focus of this Gaussian lens phase screen is approximately 0.5 wavelengths from the screen which shows good agreement with equation 4.4, and matches the results of Knepp [2].

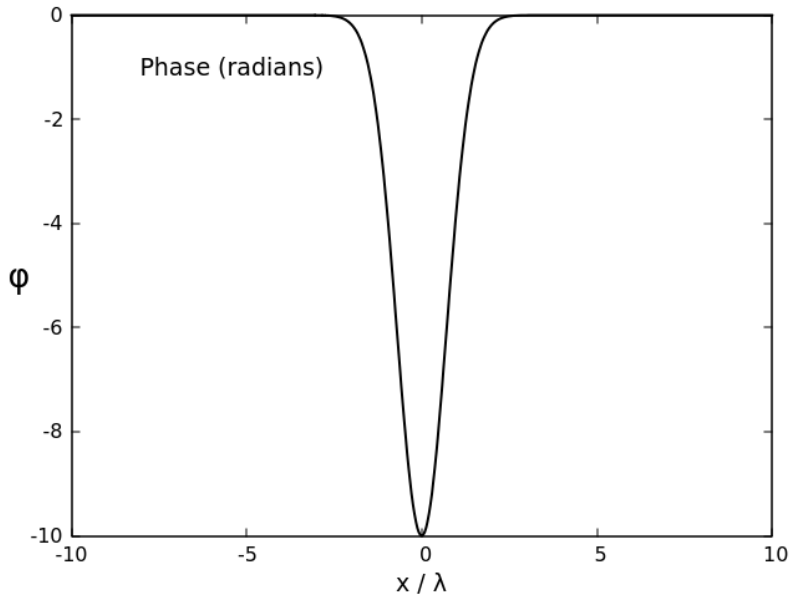

Figure 4.1: Phase contribution to plane wave at phase screen, from 4.2.

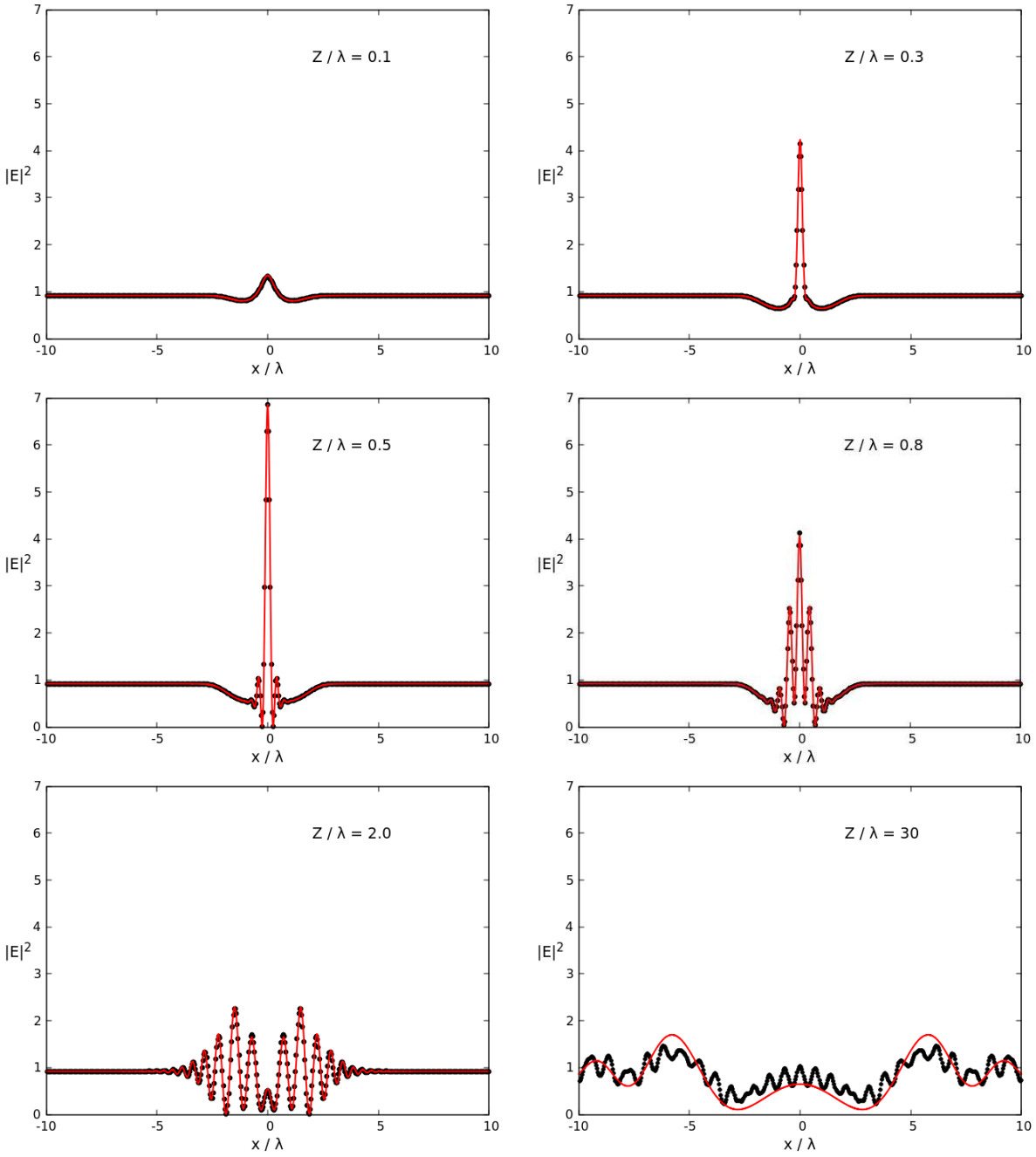

Figure 4.2: Plane wave propagation away from Gaussian lens: $|E|^2$ versus x at different distances away from the phase screen. Black dots - MPS code, Red lines - equation 4.5. Note the effect of a finite grid dimension in the MPS code at a very large distance from the grid.

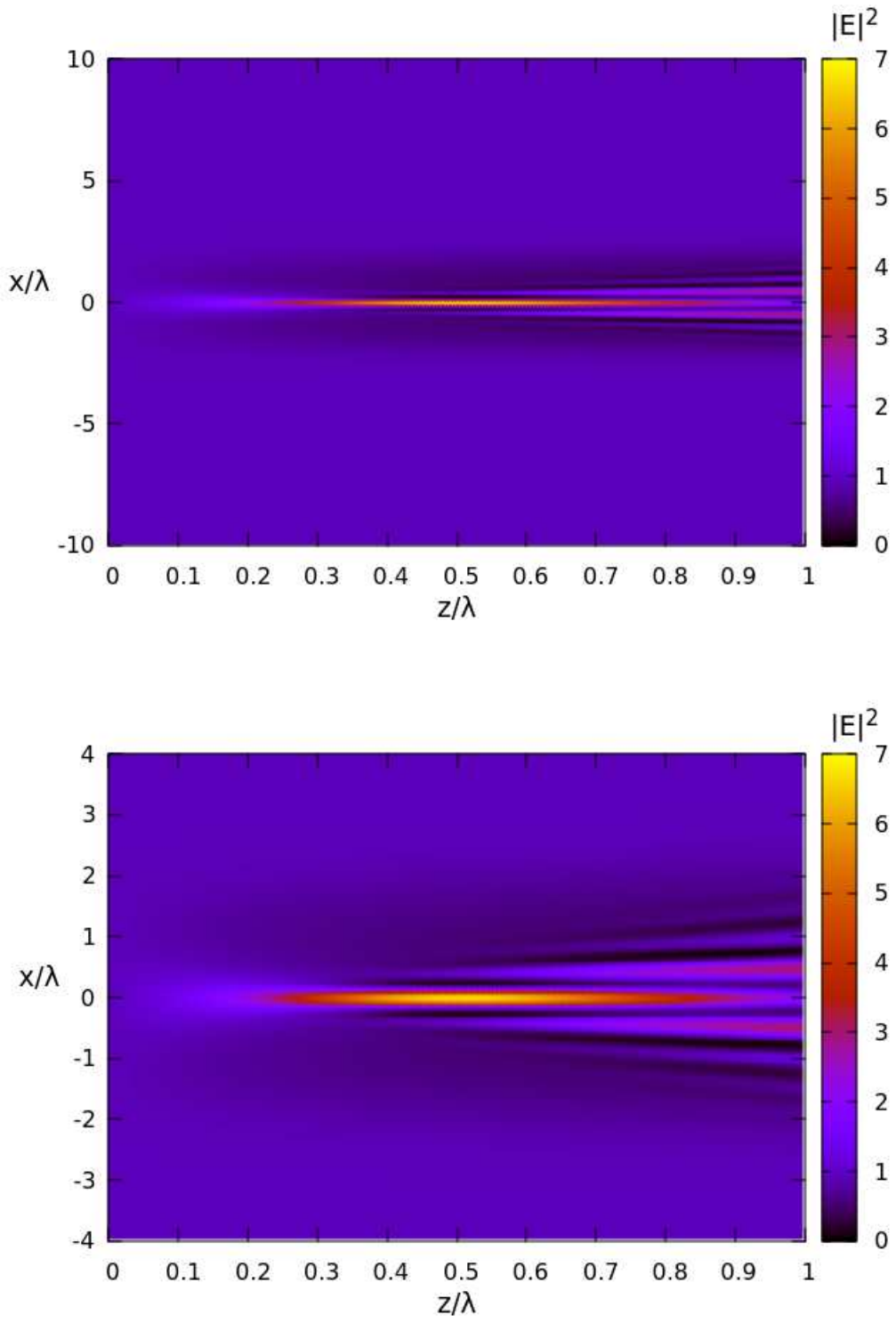

Figure 4.3: Plane wave propagation away from Gaussian lens.

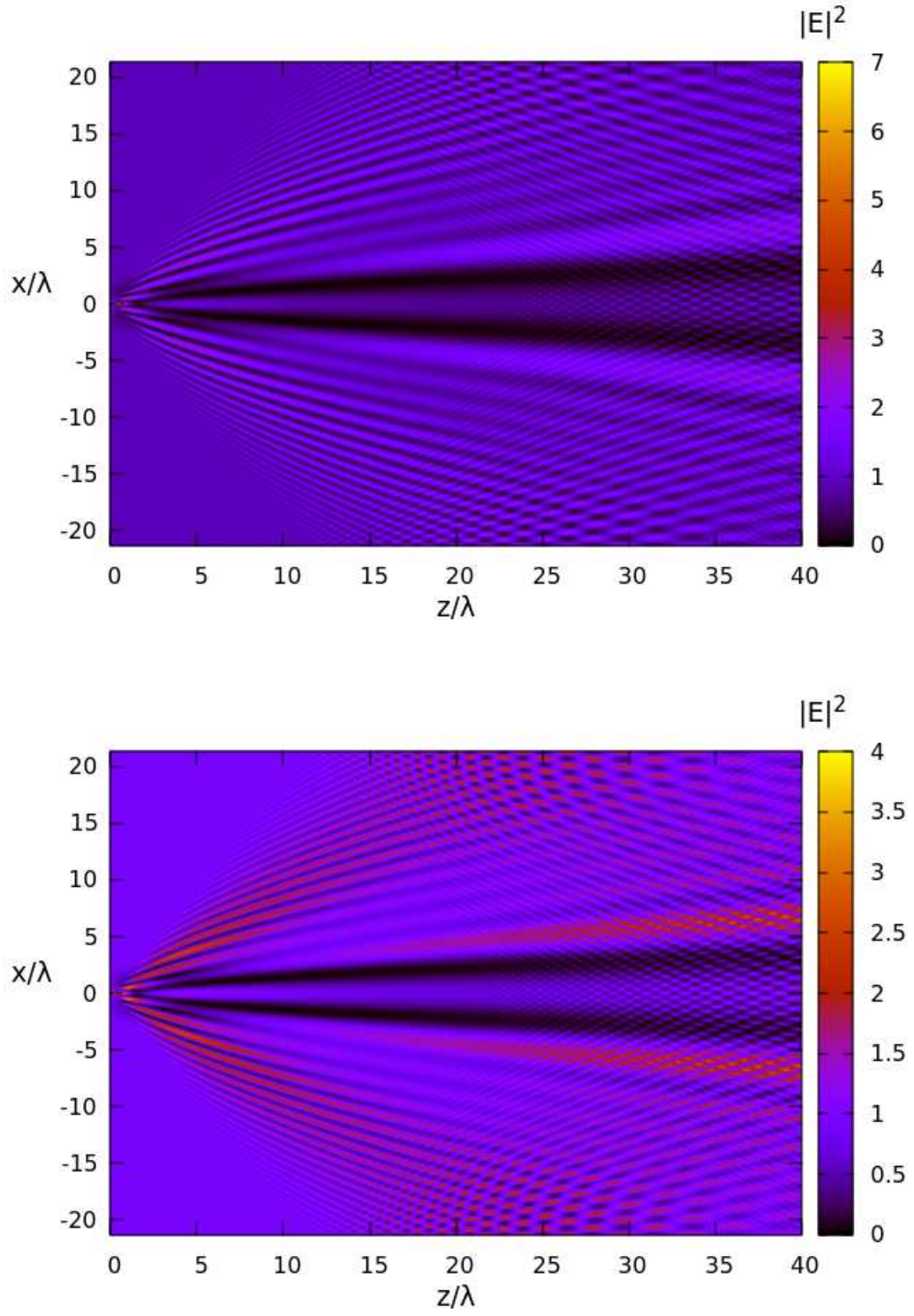

Figure 4.4: Plane wave propagation away from Gaussian lens. Effects of finite phase screen size as wave propagates away from lens. The second picture is a different scale in $|E|^2$ to better illustrate the edge effects.

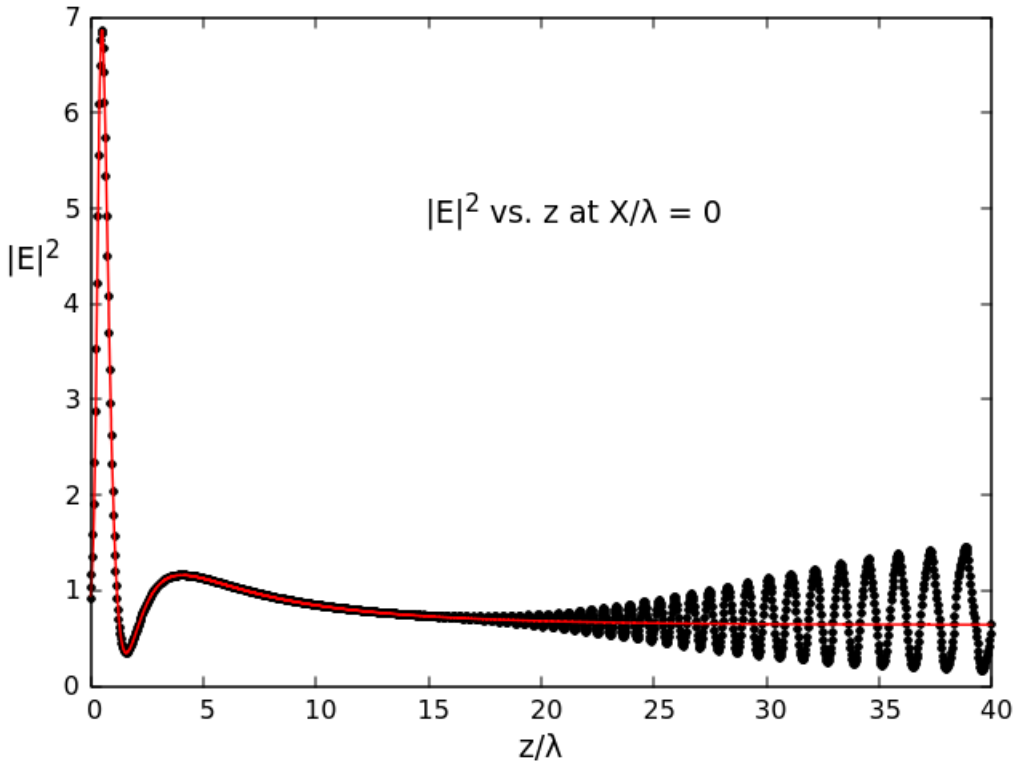

Figure 4.5: Effects of finite phase screen size as wave propagates away from lens. $|E|^2$ along the $x = 0$ axis. Black dots - MPS code, Red line - equation 4.5

4.2 Verification - Gaussian random phase screen

A second method to check the validity of the MPS code against analytic results is to propagate a single frequency wave through a phase screen with a Gaussian PSD of phase fluctuations $S_\phi(k_\perp)$ specified as

$$S_\phi(k_\perp) = \frac{\sqrt{\pi}}{2} \cdot L_0 \sigma_\phi^2 \cdot \exp\left[-k_\perp^2 L_0^2/4\right] \tag{4.6}$$

where the scale size L_0 is chosen as the wavelength λ and the phase standard deviation σ_ϕ is set to 0.1, 1, and 10 radians. The phase screen is constructed of 2048 points spaced at 0.044λ for a total length of 90.1λ.

The wave encounters the phase screen and is then observed along a receiver plane of the same perpendicular length at a number of distances away from the screen. The wave E-field $E(x, z)$ is calculated along each receiver plane.

Statistical results are obtained by running the simulation ten times, each with a different phase screen generated as in section 3.2. An individual phase screen realization for the $\sigma_\phi = 1$ case is shown in figure 4.6.

Figure 4.7, shows the difference in the numerically generated PSD, $S_{\phi,d}(k_\perp)$, and the actual PSD, $S_\phi(k_\perp)$, for the $\sigma_\phi = 1$ case. Not surprisingly, the agreement is quite good.

An additional, and arguably more important, check on the MPS code results in this case is to calculate the scintillation index S_4 from the solution to the wave electric field at distances away from the phase screen. The scintillation index is a measure of how disturbed the wave field becomes owing to the stochastic part of the propagation media (ionosphere). It is calculated from the magnitude of the wave field as

$$S_4^2 = \left\langle \frac{\left\langle \left(|E|^2 - \langle |E|^2 \rangle\right)^2 \right\rangle}{\langle |E|^2 \rangle^2} \right\rangle \tag{4.7}$$

In the weak scintillation regime S_4 can be found analytically in the thin phase screen approximation at a distance z as [17, 2]

$$S_4^2 \simeq \int_{-\infty}^{+\infty} S_\phi(k_\perp) \sin^2\left(\frac{k_\perp^2 z}{2k_0}\right) dk_\perp \tag{4.8}$$

Figure 4.8 gives the results of the MPS code compared to the calcuation in equation 4.8. For these results, the MPS code was run ten times and S_4 calculated for the ensemble of E-filed magnitudes $|E_i|$ at the center of the grid as a function of distance away from it for $\sigma_\phi = 0.1, 1$, and 10.

At small distances from the screen, and at low σ_ϕ values, the weak scattering theory applies; and the reults of the MPS code simulations bear this out quite well. at larger distances, and σ_ϕ values, weak scattering theory breaks down. The values of S_4 saturate at or near 1, which is expected based on theory and numerous measurements [11, 4].

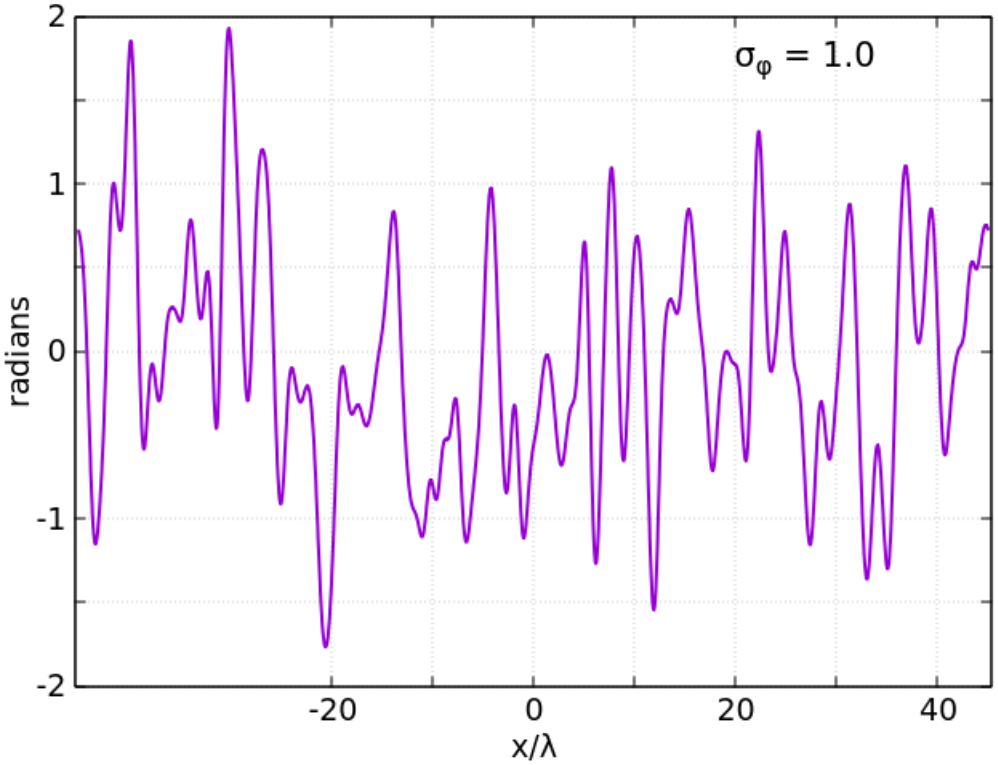

Figure 4.6: Realization of phase along the phase screen grid for a Gaussian $S_\phi(k_\perp)$.

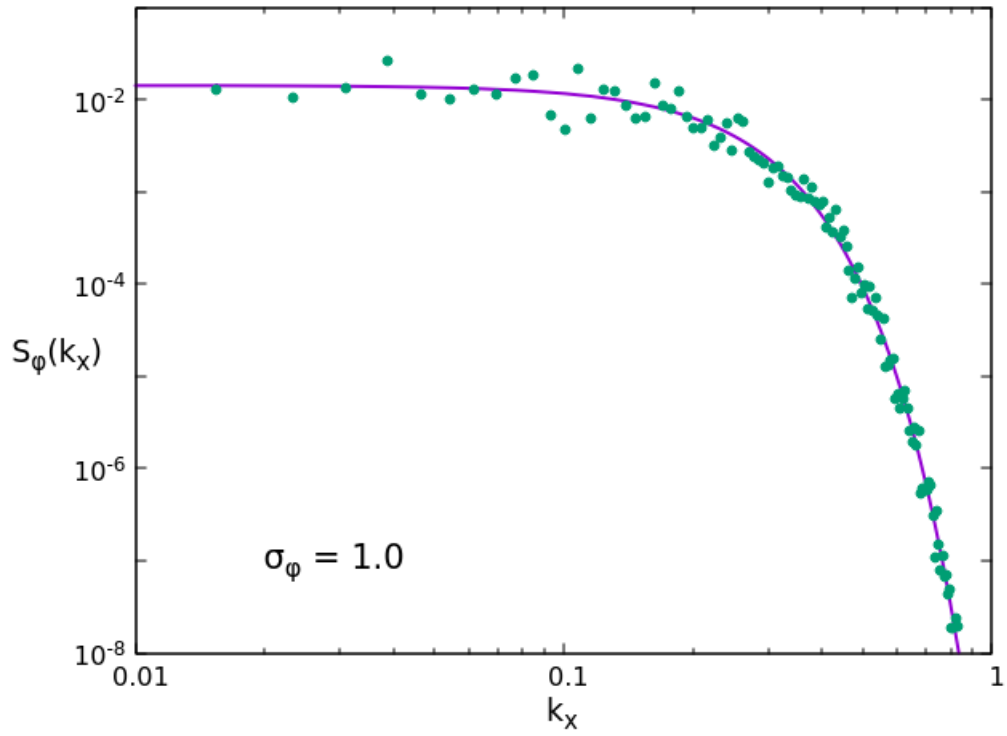

Figure 4.7: $S_\phi(k_\perp)$ (line) and $S_{\phi,d}(k_\perp)$ (points) after 10 averages, for the case $\sigma_\phi = 1$.

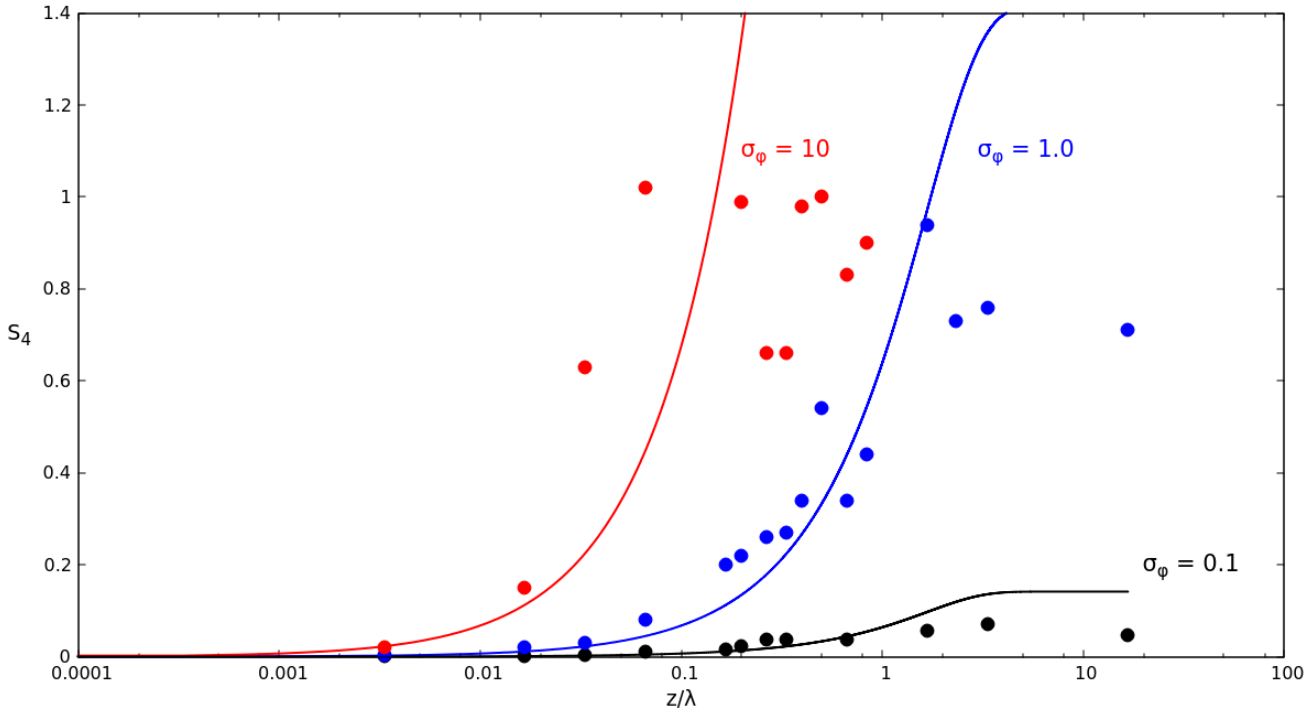

Figure 4.8: S_4 index as a function of distance away from the phase screen for a Gaussian $S_\phi(k_\perp)$. Black - $\sigma_\phi = 0.1$, Blue - $\sigma_\phi = 1$, Red - $\sigma_\phi = 10$. Lines - weak scattering theory, points - MPS model results.

4.3 Verification - code comparison using stochastic random phase screen

A last step in the verification of the MPS code was to compare the results to an existing scintillation code. It is important to re-state that all calculations in this report represent only the *stochastic* part of the ionosphere calculated from the MPS code. Mean background refraction due to the quiescent TEC background is covered by separate methods, and will not affect the stochastic parameters calculated here. We propagate a linearly chirped signal from 100 - 200 MHz (figure 4.9, top) through a single phase screen with stochastic parameters supplied by the PRPSIM code [19] and then use the same parameters in the MPS code for comparison.

Figure 4.9 shows the effects of different levels of scintillation on the original signal with $\sigma_{TEC} = 0.3$ and $\sigma_{TEC} = 50$ as modeled by the MPS code.

From the manual: "PRPSIM (Properties of Radio Wave Propagation in a Structured Ionized Medium) is a package of Fortran routines that compute statistical scintillation structure parameters and other propagation effects on radio signals propagating through high altitude ambient or nuclear disturbed environments".

The comparison was done by running the code for two the cases shown in Figure 4.9.

Figure 4.10 shows the phase PSD's for the two cases. The red lines are the PSD's supplied by PRPSIM and the black points are the numerically averaged PSD's (10 averages for $\sigma_{TEC} = 0.3$ and 30 averages for $\sigma_{TEC} = 50$). We expect very strong agreement between the two.

Figure 4.11 gives the scintillation index S_4 versus frequency over the bandwidth of the signal as calculated by both codes. We see good agreement for the mild scintillation case, but the MPS code shows more structure in the high scintillation case.

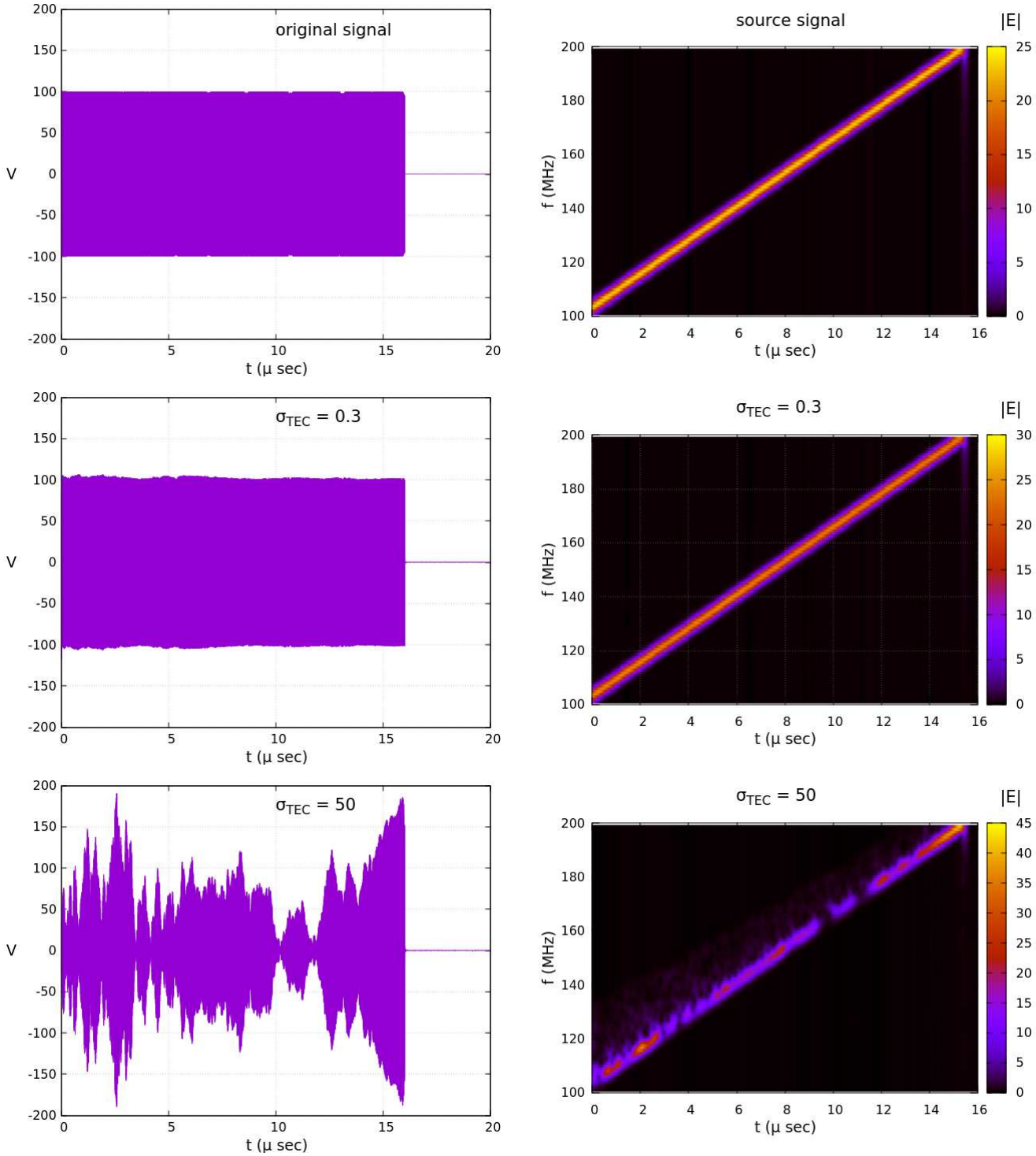

Figure 4.9: Effects of scintillation modeled by MPS code. Time waveforms and spectrograms. Top - original signal, middle - original signal through a $\sigma_{TEC} = 0.3$ phase screen, and bottom - original signal through a $\sigma_{TEC} = 50$ phase screen.

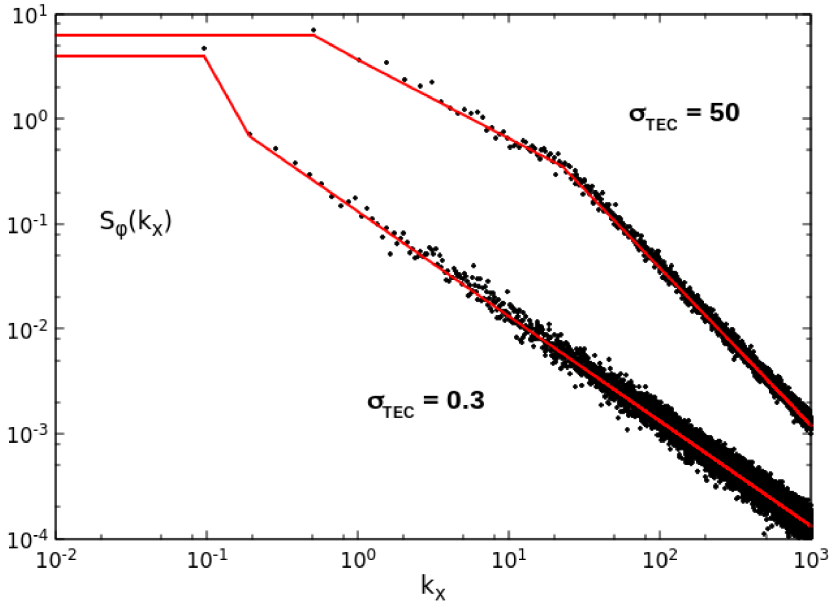

Figure 4.10: Stochastic $S_\phi(k_\perp)$ for the $\sigma_{TEC} = 0.3$, and $\sigma_{TEC} = 50$ MPS simulations. Red - specified by PRPSIM, Black - 10 averages for $\sigma_{TEC} = 0.3$ and 30 averages for $\sigma_{TEC} = 50$.

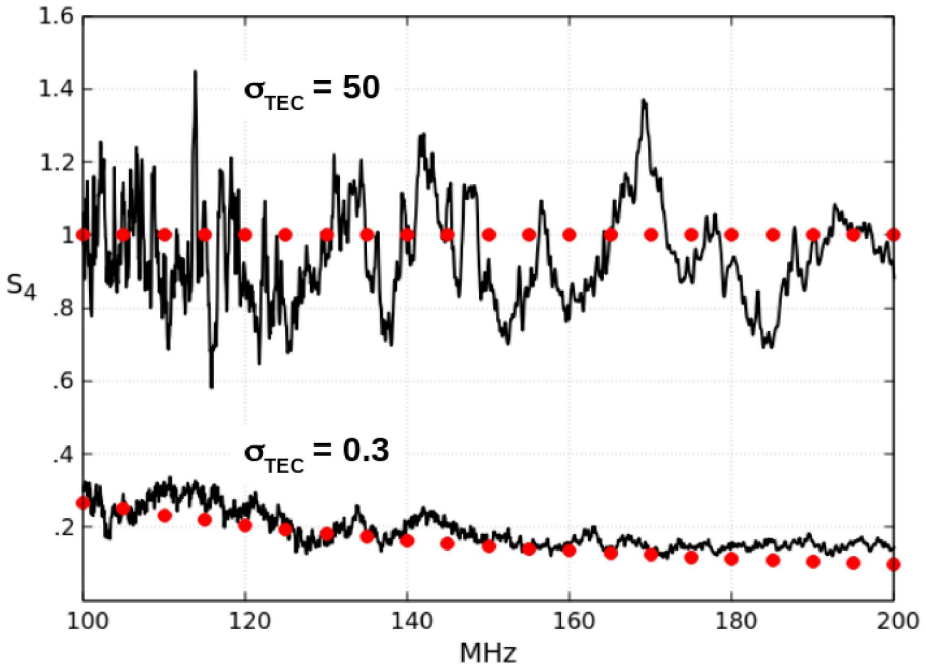

Figure 4.11: S_4 index versus frequency for the $\sigma_{TEC} = 0.3$, and $\sigma_{TEC} = 50$ Stochastic $S_\phi(k_\perp)$ MPS simulations. Red - calculated by PRPSIM, Black - calculated from the MPS code: 10 averages for $\sigma_{TEC} = 0.3$ and 30 averages for $\sigma_{TEC} = 50$.

Conclusions

We have designed and implemented a multiple phase screen code to model the effects of ionospheric irregularities on the propagation of EM signals. This code was developed using the prior work of Knepp [2].

Verification of the code using deterministic and stochastic plasma parameters shows agreement with both basic phenomenological propagation physics (sections 4.1 and 4.2) and other computer codes (section 4.3).

It is important to note that the scintillation index for a given set of stochastic ionospheric parameters can increase with increasing distance away from the screen. This is shown in equation 4.8 and in figure 4.8. Thus, we can effectively increase the S_4 by simply increasing the distance away from the screen. This has strong implications in the modeling of EM wave propagation at large distances from the phase screen, as the Nyquist conditions of section 3.3 must also be met.

In terms of trans-ionospheric EM wave propagation, it is probably best to use a single screen located at or above the maximum in the electron density profile, ensuring the most accurate statistics of ΔTEC in the phase screen.

Bibliography

[1] J. A. Ratcliffe, "Some aspects of diffraction theory and their application to the ionosphere," *Reports on Progress in Physics*, vol. 19, pp. 188–267, jan 1956.

[2] D. Knepp, "Propagation of wide bandwidth signals through strongly turbulent ionized media," Tech. Rep. DNA-TR-81-78, Defense Nuclear Agency, 03 1982.

[3] D. Knepp, "Multiple phase-screen propagation analysis for defense satellite communications system," Tech. Rep. DNA-4424T, Defense Nuclear Agency, 09 1977.

[4] C. Rino, *The Theory of Scintillation with Applications in Remote Sensing*. Wiley, 2011.

[5] K. C. Yeh and C. H. Liu, "Radio wave scintillations in the ionosphere," *Proceedings of the IEEE*, vol. 70, pp. 324–360, April 1982.

[6] J. S. Hey, S. J. Parsons, and J. W. Phillips, "Fluctuations in cosmic radiation at radiofrequencies," *Nature (London)*, vol. 158, p. 247, 1946.

[7] K. Yeh and C. Liu, *Theory of Ionospheric Waves*. International Geophysics, Elsevier Science, 1973.

[8] D. Swanson, *Plasma Waves, 2nd Edition*. Series in Plasma Physics, Taylor & Francis, 2003.

[9] T. Stix, *Waves in Plasmas*. American Inst. of Physics, 1992.

[10] K. Budden, *Radio Waves in the Ionosphere*. Cambridge University Press, 1961.

[11] A. Wheelon, *Electromagnetic Scintillation: Volume 1, Geometrical Optics*. Cambridge University Press, 2001.

[12] "NRL plasma formulary." NRL Publication number 177-4405, 1990.

[13] F. Stremler, *Introduction to Communication Systems*. Addison-Wesley, second ed., 1982.

[14] A. Papoulis, *Probability, Random Variables, and Stochastic Processes*. McGraw Hill, 1965.

[15] C. Carrano. Private communication.

[16] D. Knepp, "Multiple phase-screen calculation of the temporal behavior of stochastic waves," *Proceedings of the IEEE*, vol. 71, pp. 722 – 737, 07 1983.

[17] E. E. Salpeter, "Interplanetary scintillations. I. theory," *Astrophysical Journal*, vol. 147, pp. 433 – 448, 1967.

[18] R. Buckley, "Diffraction by a random phase-changing screen: A numerical experiment," *Journal of Atmospheric and Terrestrial Physics*, vol. 37, pp. 1431–1446, 1975.

[19] R. E. Dodson, D. J. Krueger, and F. W. Guigliano, "PRPSIM - a fortran code to calculate properties of radio wave propagation in a structured ionized mediumn," Tech. Rep. MRC-R-1011, Mission Research Corporation, 1989. https://apps.dtic.mil/dtic/tr/fulltext/u2/a216299.pdf.